Technical Annals

Vol 1, No 7 (2024)

Technical Annals

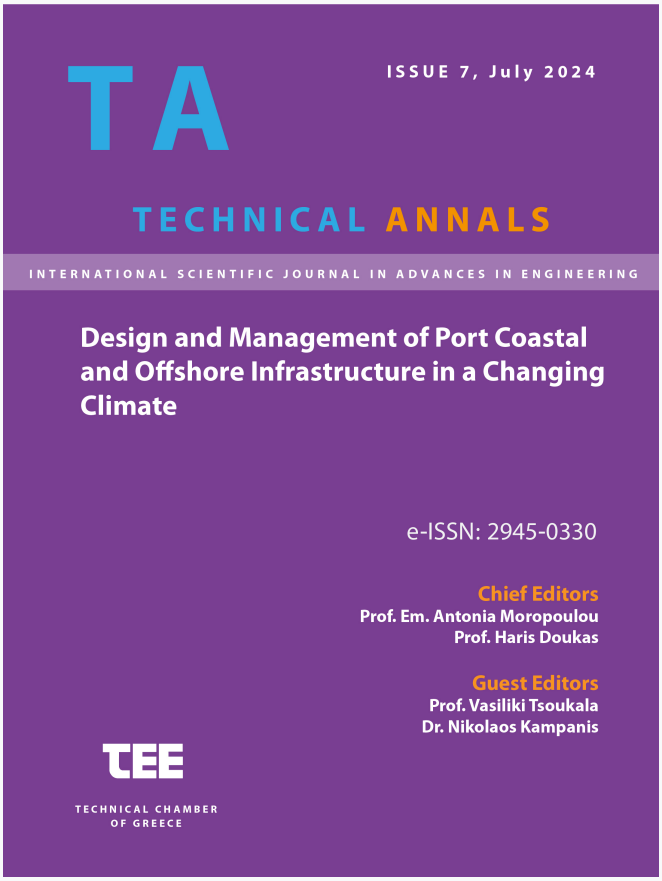

Hydrodynamic Load Benchmarking on Bottom-Seated Cylinders in Finite Depths: A Frequency-Domain Comparison of Analytical and Open-Source BEM Solutions

Sarantos Sarantidis, Thomas P. Mazarakos

doi: 10.12681/ta.40045

To cite this article:

Sarantidis, S., & Mazarakos, T. P. (2024). Hydrodynamic Load Benchmarking on Bottom-Seated Cylinders in Finite Depths: A Frequency-Domain Comparison of Analytical and Open-Source BEM Solutions. *Technical Annals*, *1*(7). https://doi.org/10.12681/ta.40045

Hydrodynamic Load Benchmarking on Bottom-Seated Cylinders in Finite Depths: A Frequency-Domain Comparison of Analytical and Open-Source BEM Solutions.

Sarantos P. Sarantidis[1][0009-0005-5446-7073] and Thomas P. Mazarakos[1][0000-0001-5317-2656]

[1]Department of Naval Architecture, School of Engineering, University of West Attica, Campus 1, Ag. Spyridonos 28, 12241 Egaleo, Attica, Greece
ssarantidis@uniwa.gr, tmazar@uniwa.gr

Abstract. The scope of the presented paper is a benchmark study between the results of analytical and Boundary Element Method (BEM) solutions for the hydrodynamic problem of a vertical fixed cylinder due to the action of linear waves. First-order hydrodynamic exciting wave forces and moments, added mass, hydrodynamic damping coefficients, and the Response Amplitude Operators (RAOs) for the surge motion are calculated. The mean second-order wave drift forces are also given by using the direct integration method. The analytical solution is calculated in the frequency domain for a wide range of frequencies for different cylinder characteristics. Finite water depths and linear waves are considered. Therefore, a formulation of the problem based on the Laplace equation and boundary conditions on the free surface and seabed, is given. Also, two different open-source BEM codes are used to solve the hydrodynamic problem. The calculated results are compared to those of other investigators' analytical and numerical predications.

Keywords: Exciting wave forces, added mass, hydrodynamic damping, mean second-order wave drift forces, RAOs, analytical solution, BEM methods.

1 Introduction

Each offshore structure resting on vertical legs (cylinders) fixed to the installation seabed, is subjected to external loads and motions due to the external operating conditions such as wind [1], sea waves, and sea currents [2]. These loads and motions affect the stability and safety of structures. Therefore, it is crucial to proceed with analytical calculations in order to obtain these values. Through the years, many researchers have been involved with the estimation of the hydrodynamic loads acting on floating structures. In the literature, a series of analytical and semi-analytical solutions for the solution of the scattering problem and the calculation of the external loads (first and mean second-order wave forces) on floating bodies of different shapes, at a wave incidence, have been presented.

Haskind [3] was the first – one who solved the hydrodynamic problem of a ship surface due to wave incident, by solving the radiation problem. Based on the linear

hydrodynamic theory of ship oscillations in the presence of linear waves, he determined the velocity potential equation, the corresponded boundary conditions it must satisfy and stated that the hydrodynamic forces and moments acting on ship surface are solely due to ship radiation functions that define how waves are generated in a dense fluid when the ship oscillates at a unit velocity in still water.

Then Maruo [4] developed the general equations for the horizontal surge and sway drift forces acting on floating objects in deep water by using the momentum method. These equations were based on the far-field velocity potential of the object, being represented through Kochin functions.

Newman [5] developed analytical expressions for the exciting forces and moments acting on fixed bodies of arbitrary shape at a wave incident. He based on the Haskind equations to determine the asymptotic velocity potential at a large distance of the body (crucial for the calculation of the hydrodynamic forces) and the near field velocity potential for the hydrodynamic problem of a submerged ellipsoid and a floating two-dimensional ellipse at a wave incident. Then in a subsequent study [6] he derived the Maruo and Suyehiro equations for the calculation of the drift forces and moments (respectively) on the surface of a slender ship. The analytical numerical results were compared to those of the experimental study of a series 60 hull form and a good agreement at small values of wave length was confirmed.

Hess and Smith [7] were the first who involved the so-called panel method in the potential problem while Garrett [8] developed his analytical procedure for the calculation of the exciting forces acting on a circular dock based on the Galerkin's method. Bai [9] utilized a two-dimensional finite element approach to calculate the forces generated by wave excitation, along with the reflection and transmission coefficients, for oblique waves interacting with various structures. These structures included a vertical flat plate, a horizontal flat plate, and rectangular cylinders. Through this method, Bai was able to analyze how the waves behaved when they encountered these different objects, providing insight into the effects of wave interaction on their surfaces.

Pinkster and Oortmersen [10] presented their own work on the calculation of the first-order exciting wave forces by using a singularity distribution on the wetted surface of the body in its equilibrium position as well as the mean second-order wave forces acting on floating bodies with the aim of the direct integration method. The analytical numerical results were compared to those of corresponding model tests with a satisfied convergence. Rahman and Bhatta [11] used an eigenfunction expansion for the solution of the linear radiation problem in order to obtain the added mass and damping coefficients for a vertical surface-piercing circular cylinder extending to the seabed and undergoing horizontal oscillations.

Mavrakos [12] determined the mean drift loads for a configuration of multiple hydrodynamically interacting cylinders by applying the principle of momentum conservation. This was done by defining appropriate control fluid volumes around each cylinder in the multi-body system. Finally, Mansour et. al [13] proposed a Boundary Integral Method (BIM) for the solution of the hydrodynamic problem of vertical cylinder fixed to the seabed, extending through the water surface in a region with a finite water depth.

In order to estimate the motions of a floating body, the radiation problem need to be solved. By linearizing the governing equations (Laplace equation and boundary conditions on the seabed and surface) the problem is simplified and then the added mass and the hydrodynamic damping coefficients are extracted [11]. Following that, the Response Amplitude Operators (RAOs) are obtained [5].

In this paper, the incident, diffraction and radiation problem of a simple bottom-seated vertical cylinder, at a linear wave (Airy) incidence, in a water area of finite depth is solved with the aim of the Laplace equation and the appropriate linearized boundary conditions on the seabed, water surface and cylinder's wetted surface. The general equations of the exciting forces and moments are obtained by calculating the pressure field around the cylinder. Then the added mass, the hydrodynamic damping, and the Response Amplitude Operators (RAO's) for the surge motion are evaluated. Also, the mean second-order wave drift forces are estimated by using the direct integration method (or near field method) [14]. A body surface mesh parametric analysis is conducted for the purpose of determining the optimum mesh geometry for the simulations with the aim of BEM methods. This analysis is performed to ensure the minimum divergence, and the results are compared with analytical solutions [15]. The results are compared with two open-source codes based on BEM methods, NEMOH [16, 17, 18, 19, 20] and HAMS [21, 22].

2 Theoretical Background

In Fig. 1-2 the characteristics of the examined vertical fixed cylinder of finite length, the characteristics of the wave incident and the water area, that cylinder is set in, are shown. The exciting and mean second-order wave drift forces, the added mass, the hydrodynamic damping and the RAO's acting on the body are obtained by solving the corresponding diffraction and radiation problem.

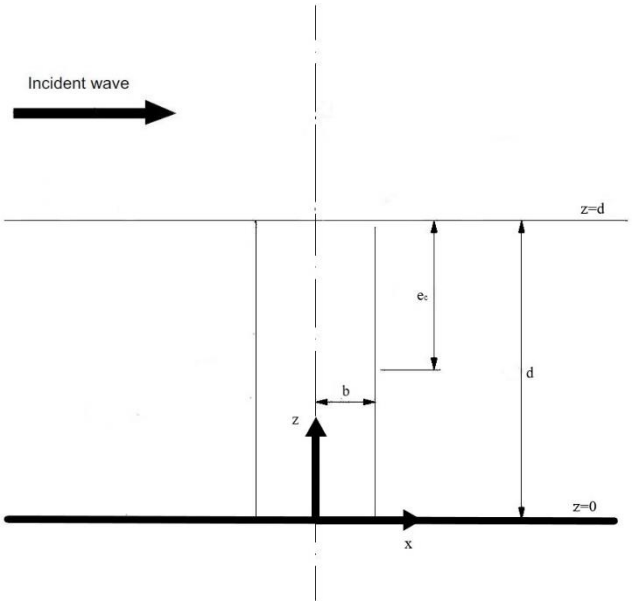

Fig. 1. Coordinate system for the vertical bottom-seated cylinder (side view).

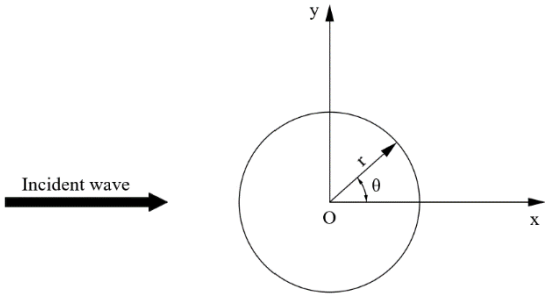

Fig. 2. Coordinate system for the vertical bottom-seated cylinder (top view).

The incident velocity potential of the simple harmonic wave is given in cylindrical coordinates by Mei [23]:

$$\varphi^I = -i\omega \frac{H}{2} \frac{cos\, h(kz)}{ksinh(kd)} \sum_{m=0}^{\infty} \varepsilon_m\, i^m\, J_m\,(kr)\cos(m\theta) \tag{1}$$

where:
i = imaginary unit
ω = wave angular frequency, given by the dispersion equation $\omega^2 = kgtanh(kd)$
g = acceleration of gravity
k = wave number
ε_m = Neumann constant, equal to 1, for m=0 and equal to 2 for m≥1
J_m = Bessel function of first-kind and m^{th} order

(r, θ, z) = cylindrical coordinates

while the diffraction velocity potential around the cylinder-wetted surface, from the seabed to the free surface, is given in cylindrical coordinates by MacCamy & Fuchs [24]:

$$\varphi^D = i\omega \frac{H}{2} \frac{\cosh(kz)}{k\sinh(kd)} \sum_{m=0}^{\infty} \varepsilon_m i^m \frac{J'_m(kb)}{H'_m(kb)} H_m(kr) \cos(m\theta) \tag{2}$$

where:
H_m= Hankel function of first-kind and m^{th} order

The total velocity potential is given by the sum of the incident and diffraction velocity potential:

$$\varphi = \varphi^I + \varphi^D = -i\omega \frac{H}{2} \frac{\cosh(kz)}{k\sinh(kd)} \sum_{m=0}^{\infty} \varepsilon_m i^m \left(J_m(kr) - \frac{J'_m(kb)}{H'_m(kb)} H_m(kr) \right) \cos(m\theta) \tag{3}$$

2.1 Exciting Wave Forces and Moments

The exciting wave forces on the body are evaluated by the integration of the pressure field, which, according to the linear wave theory, must fulfil the Bernoulli's equation:

$$p = -\rho \frac{\partial \Phi}{\partial t} = i\omega\rho\varphi e^{-i\omega t} \tag{4}$$

where:
ρ = water density

The first-order horizontal exciting wave force on the body is given by [25]:

$$F = -\iint_S p\vec{n}dS \tag{5}$$

where:
S = floating body wetted surface.
$\vec{n}$ = the unit normal vector pointing outward to the body's surface S.

The analytical representation for the first-order horizontal exciting wave force is given by the following equation [15]:

$$F_x = \rho g b^2 \left(\frac{H}{2}\right) \frac{4\tanh(kd)}{(kb)^2 H'_1(kb)} \tag{6}$$

The first-order exciting wave moment on the vertical fixed cylinder is given by the following equation [15]:

$$My = -\iint_S p(z - \mathrm{e}_c)\cos\theta dS \tag{7}$$

The analytical representation for the first-order exciting wave moment is given by the following equation:

$$My = \rho g b^3 \left(\frac{H}{2}\right) \frac{4}{(kb)^3 \cosh(kd)\, H'_1(kb)} (kd\sinh(kd) + 1 - \cosh(kd)) - \mathrm{e_c} F_x \tag{8}$$

where:

$\mathrm{e_c}$: vertical position of the center of gravity, measured from the free surface

2.2 Added Mass, Hydrodynamic Damping and RAOs

Formulation of the hydrodynamic problem follows closely that of the diffraction problem. The radiated waves will replace the incident waves, therefore, using Rahman and Bhatta formulation [11], the added mass A_{11} and damping coefficient B_{11} are obtained from the radiation potential φ_R as defined by:

$$A_{11} - \frac{i}{\omega} B_{11} = \rho \int_S \varphi_R \cos\theta dS \tag{9}$$

The real part and the imaginary part of equation (9) can be expressed:

$$A_{11} = Re\left\{\rho \int_S \varphi_R \cos\theta dS\right\} \tag{10}$$

and

$$B_{11} = Im\left\{\rho\omega \int_S \varphi_R \cos\theta dS\right\} \tag{11}$$

After extensive mathematical calculations the following analytical expression for the added mass and the hydrodynamic damping, respectively is obtained.

The analytical representation for the added mass and hydrodynamic damping coefficients are given by the following equations [11]:

$$A_{11} = -\rho b^3 \pi \times \left[\frac{k \sinh^2(kd)}{(kb)^2 k^2 \frac{d}{2}\left(1 + \frac{\sinh(2kd)}{2kd}\right)} Re\left(\frac{H_1(kb)}{H'_1(kb)}\right) + \sum_{j=1}^{\infty} \frac{k_j \sinh^2(k_j d)}{(k_j b)^2 k_j^2 \frac{d}{2}\left(1 + \frac{\sinh(2k_j d)}{2k_j d}\right)} \frac{K_1(k_j b)}{K'_1(k_j b)}\right] \tag{12}$$

$$B_{11} = -\rho b^3 \omega \pi \frac{k \sinh^2(kd)}{(kb)^2 k^2 \frac{d}{2}\left(1 + \frac{\sinh(2kd)}{2kd}\right)} Im\left(\frac{H_1(kb)}{H'_1(kb)}\right) \tag{13}$$

where:

H_1= 1^{st} order Hankel function of first-kind

K_1= 1^{st} order Modified Bessel function of second-kind

k_j= real positive solutions of the equation $\omega^2 = -k_j g \tan(k_j d)$

It was found that taking $j = 10$ number of roots produced results accurate to four significant digits.

The equation of surge motion is given by [5]:

$$x(\omega)[-\omega^2(M + A_{11}) + i\omega B_{11}] = F_x \tag{14}$$

where:
M: mass of the cylinder

Solving for the surge displacement $x(\omega)$:

$$x(\omega) = \frac{F_x}{-\omega^2(M + A_{11}) + i\omega B_{11}} \tag{15}$$

The RAO of surge motion is given by the following equation:

$$RAO_X = \frac{x(\omega)}{H/2} \tag{16}$$

Combining Eq. (15) and Eq. (16) we finally get:

$$RAO_X = \frac{F_x \,/\, (H \,/\, 2)}{-\omega^2(M + A_{11}) + i\omega B_{11}} \tag{17}$$

2.3 Mean Second-Order Wave Drift Forces

Considering the calculation of the mean second-order wave drift forces of a floating body at a wave incident, two methods have been developed: the direct integration method or near field method [10], in which all the terms of the hydrodynamic pressure on the instantaneously wetted surface, involved in second-order loads, are directly integrated and the momentum conservation principle or far field method ([4], [12], [6]) in which the knowledgeable of the potential velocity in a great distance from the body is needed. In this paper, the calculation of the mean second-order wave drift forces will be occurred with the aid of the direct integration method but the corresponding numerical results of the analytical solution [15] and the computational program NEMOH that compared to the presented analytical solution have been calculated with the momentum conservation principle method.

The analytical expression of the total wave drift force acting on the vertical-fixed cylinder is given as follows [15]:

$$F_{xd} = \frac{\rho}{4}\left\{\iint \nabla\varphi\nabla\bar{\varphi}n_j dS + \frac{\omega^2}{g}\int \varphi\bar{\varphi}n_j d\Gamma\right\} \tag{18}$$

After some manipulation, the analytical representation of the horizontal wave drift force is given by the following equation [26]:

$$F_{xd} = \frac{\rho g b (H/2)^2}{\pi(kb)^2}\left(1 + \frac{2kd}{sinh\, 2kd}\right) Re \sum_{m=-\infty}^{\infty}\left(\frac{m(m+1)}{(kb)^2} - 1\right)\frac{-i}{\overline{H'_{m+1}}(kb)H'_m(kb)} \tag{19}$$

The asterisk denotes the complex conjugate and the i denotes the imaginary part of the complex number. It was found that taking $m = [-6, 6]$ leads to numerical results with four significant digits accuracy.

2.4 BEM Methods

NEMOH

NEMOH v.3 [16, 17] is an open-source code for the calculation of the hydrodynamic exciting forces and moments acting on floating structures, as well as the first-order hydrodynamic coefficients (added mass, hydrodynamic damping, exciting wave forces) in the frequency domain. Its computational structure is based on the linear wave theory with a principle of a non-viscid fluid and non-rotational and non-compressible flow. The latest version of the code concludes the removal method for the treatment of the irregular frequencies, an extended module to post-process the first-order hydrodynamic results and an extended module for computing difference- and sum- frequencies Quadratic Transfer Functions (QTFs) for fixed or floating bodies [18, 19, 20]. The Response Amplitude Operators for the six motions of the body are also calculated. The discretization of the floating body is occurred with either the aid of the code itself (only half of the body surface if symmetry occurs) or the aid of CAD program (the whole body surface).

HAMS

HAMS [21, 22] is an open-source software for the analysis of wave diffraction and radiation hydrodynamic problem of offshore floating structures. Like NEMOH, it calculates the hydrodynamic loads and hydrodynamic coefficients by solving the boundary integral equations based on the linear wave theory with a principle of a non-viscid fluid and non-rotational and non-compressible flow.

The code can remove the irregular frequencies by an appropriate adjustment to the Control file and it has been optimized for modeling, thus it is fast, with great computational accuracy. The discretization of the floating body is occurred with the aid of CAD program.

3 Results

The extracted numerical results of the above Equations are plotted and compared against the wave angular frequency ω along with the corresponding results of the open-source codes NEMOH [16, 17] and HAMS [21, 22] and the analytical solutions of [15] for three different cylinder cases (Table 1). It has to be mentioned that the discretization of the whole body surface for both the open-source codes is occurred with the aid of CAD program (see Fig. 3 and 4). The number of elements referred to the mesh grid for the discretization of only the wetted surface of the body in each case study. However, for the hydrodynamic calculations with the aim of HAMS [21, 22], the waterline surface also needs to be discretized (as opposed to the hydrodynamic calculations with the aim of NEMOH [16, 17]). The number of elements for the discretization of the waterline surface in each case study is shown in Table 1, next to the number of elements for the discretization of the wetted surface, between brackets.

Table 1. Cylinder cases.

Cylinder Characteristics	Number of elements
Case study 1: $b = 10\ m, d = 10\ m, \mathrm{e_c} = 5\ m$	600 (476)
Case study 2: $b = 10\ m, d = 30\ m, \mathrm{e_c} = 15\ m$	900 (252)
Case study 3: $b = 10\ m, d = 50\ m, \mathrm{e_c} = 25\ m$	2000 (336)

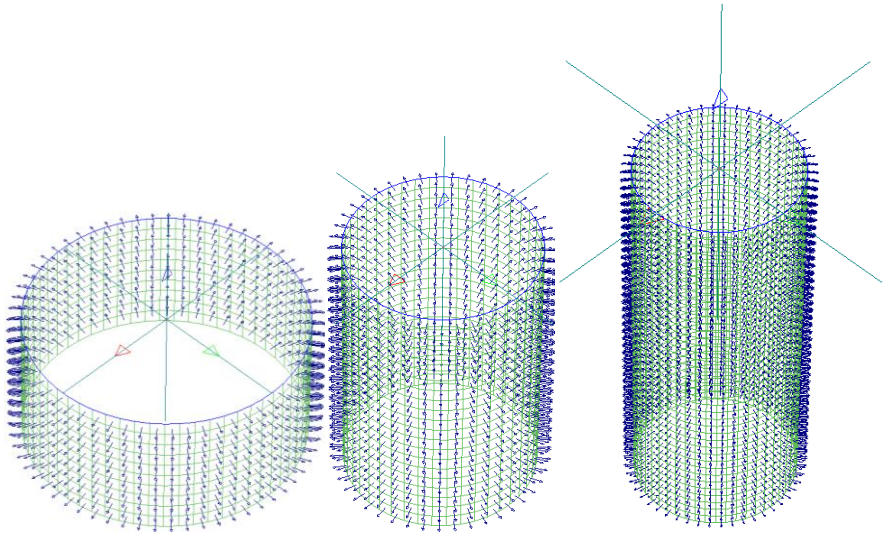

Fig. 3. Panel discretization for case study 1(left), 2 (center) and 3 (right) in NEMOH.

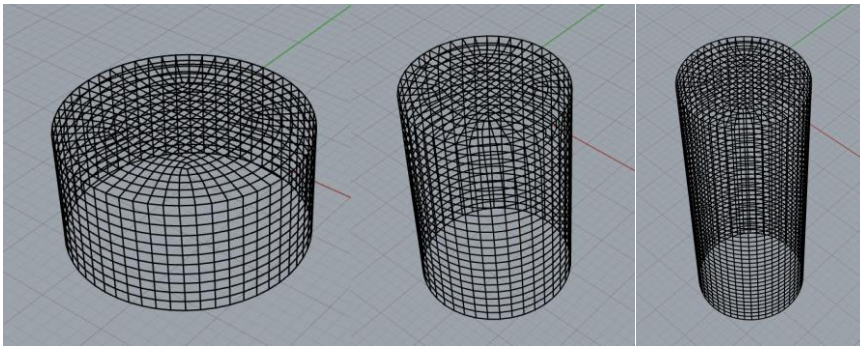

Fig. 4. Panel discretization for case study 1(left), 2 (center) and 3 (right) in HAMS.

Determined the mesh grid characteristics for body wetted surface discretization is a crucial part for the hydrodynamic calculations with the aim of the BEM methods. Body's geometry complexity and the open-source code capabilities are mainly the two

factors that affects the discretization of the body surface. One criterion that determines the quality of the constructed body mesh is the deviation of the numerical results of the BEM methods to those of a proposed numerical analytical solution for the calculation of a specific hydrodynamic magnitude. The smaller the deviation the better the quality and therefore the more accurate the mesh characteristics to be selected (number of panels/elements, shape of panels). That concludes to the fact that the optimum mesh grid is selected and therefore the accuracy of the BEM methods is assured for the calculation of the rest hydrodynamic magnitudes. Finally, a basic information is retained for the determination of the mesh grid for the discretization of larger and more complex body geometries. The exciting wave force Fx was selected in the current analysis as a criterion for the BEM methods computational accuracy and the quality of the body mesh grid.

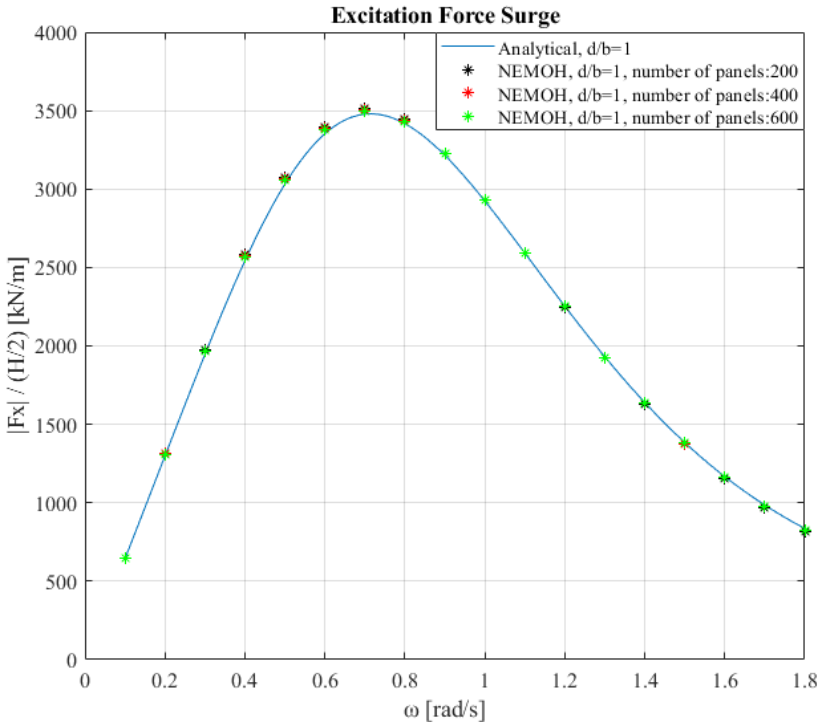

Fig. 5. Horizontal exciting force F_x versus ω for $d/b = 1$, for different numbers of body surface discretization elements for the calculations with the aim of the NEMOH.

In Fig. 5 the numerical results of the analytical solution and the open-source code NEMOH for different numbers of body surface discretization elements ($200, 400$ and 600), for the exciting wave force Fx are plotted against the wave angular frequency ω, for Case study 1. For wave angular frequency $0.5 < \omega < 0.9$ values and for wave angular frequency values ($\omega > 1.3$ rad/s) a discretization with small number of elements leads to overestimated and underestimated values of the exciting wave force Fx (compared to the corresponding analytical solution results) respectively. Therefore a total

of 600 quadrilateral elements have been used for the discretization of the body's wetted surface for ratio d/b equal to 1, in the case of the open-source code NEMOH calculations (see Fig. 3).

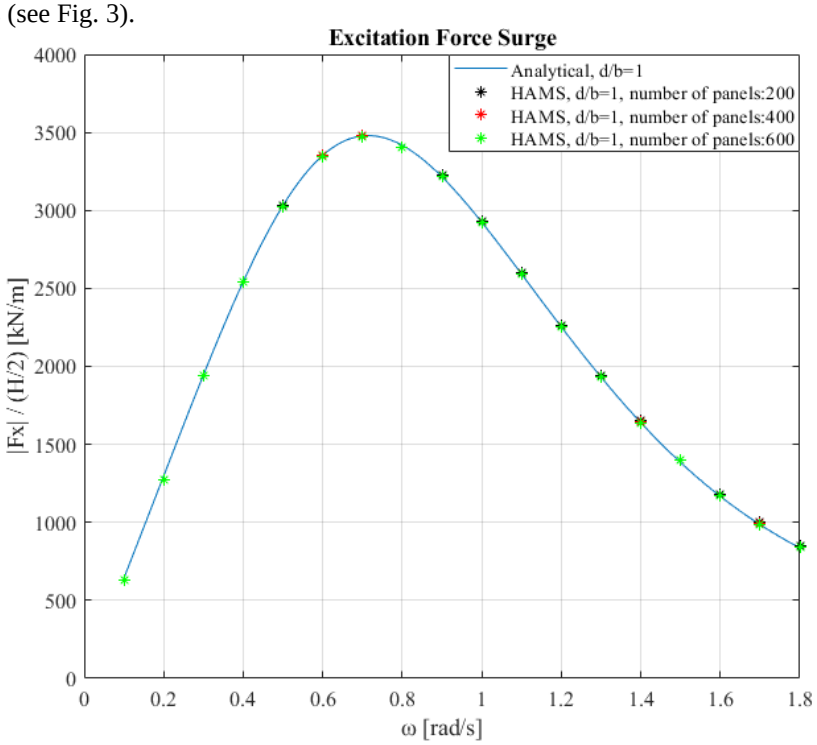

Fig. 6. Horizontal exciting force F_x versus ω for $d/b = 1$, for different numbers of body surface discretization elements for the calculations with the aim of the HAMS.

In Fig. 6 the numerical results of the analytical solution and the open-source code HAMS for different numbers of body surface discretization elements (200,400 and 600), for the exciting wave force Fx are plotted against the wave angular frequency ω, for Case study 1.

The body surface discretization cases studied in the case of the open-source code NEMOH calculations are also studied in the case of the open-source code HAMS calculations, in order to compare the computing precision of the two codes. At small values of wave angular frequency ω the number of body surface discretization elements doesn't affect the calculating precision of the open-source code HAMS. However, for larger values of wave angular frequency ($\omega > 1.5$ rad/s) a discretization with small number of elements leads to overestimated values of the exciting wave force Fx (compared to the corresponding analytical solution results). Therefore a total of 600 quadrilateral elements have been used for the discretization of the body's wetted surface for ratio d/b equal to 1, in the case of the open-source code HAMS calculations (see Fig. 4).

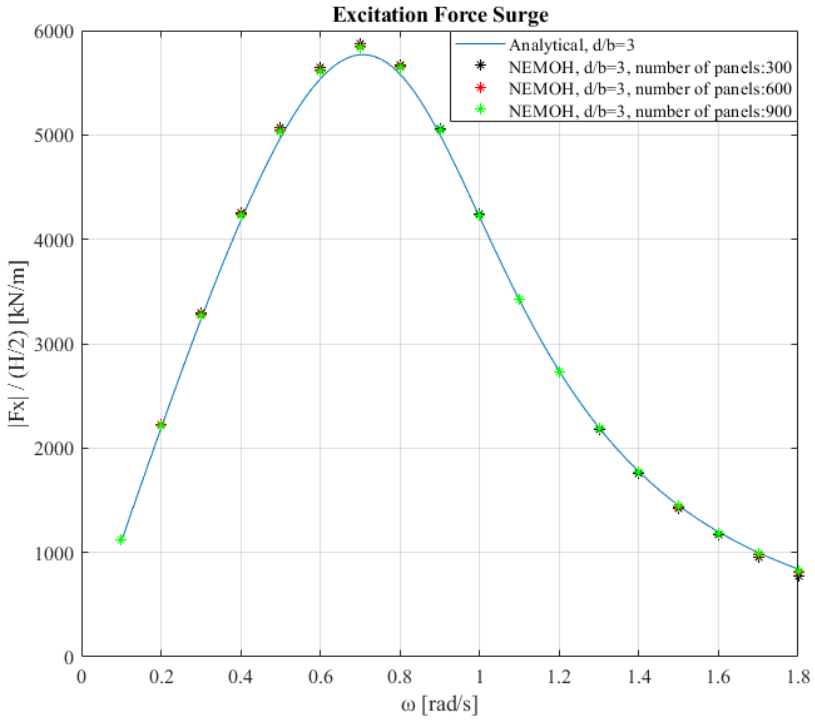

Fig. 7. Horizontal exciting force F_x versus ω for $d/b = 3$, for different numbers of body surface discretization elements for the calculations with the aim of the NEMOH.

In Fig. 7 the numerical results of the analytical solution and the open-source code NEMOH for different numbers of body surface discretization elements ($300, 600$ and 900), for the exciting wave force Fx are plotted against the wave angular frequency ω, for Case study 2. Considering the body surface increase, a larger number of elements for the different studied discretization cases is selected.

For wave angular frequency $0.4 < \omega < 1$ values and for wave angular frequency values ($\omega > 1.3$ rad/s) a discretization with small number of elements leads to overestimated and underestimated values of the exciting wave force Fx (compared to the corresponding analytical solution results) respectively. Therefore a total of 900 quadrilateral elements have been used for the discretization of the body's wetted surface for ratio d/b equal to 3, in the case of the open-source code NEMOH calculations (see Fig. 3).

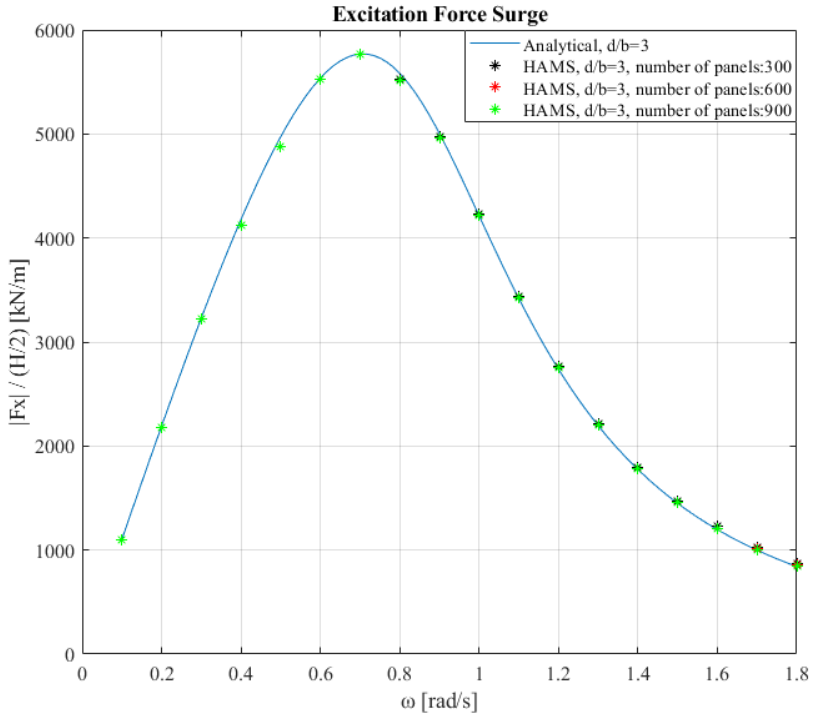

Fig. 8. Horizontal exciting force F_x versus ω for $d/b = 3$, for different numbers of body surface discretization elements for the calculations with the aim of the HAMS.

In Fig. 8 the numerical results of the analytical solution and the open-source code HAMS for different numbers of body surface discretization elements ($300, 600$ and 900), for the exciting wave force Fx are plotted against the wave angular frequency ω, for Case study 2. The body surface discretization cases studied in the case of the open-source code NEMOH calculations are also studied in the case of the open-source code HAMS calculations, in order to compare the computing precision of the two codes. For wave angular frequency values ($\omega > 1.2$ rad/s) a discretization with small number of elements leads to overestimated values of the exciting wave force Fx (compared to the corresponding analytical solution results). Therefore a total of 900 quadrilateral elements have been used for the discretization of the body's wetted surface for ratio d/b equal to 3, in the case of the open-source code HAMS calculations (see Fig. 4).

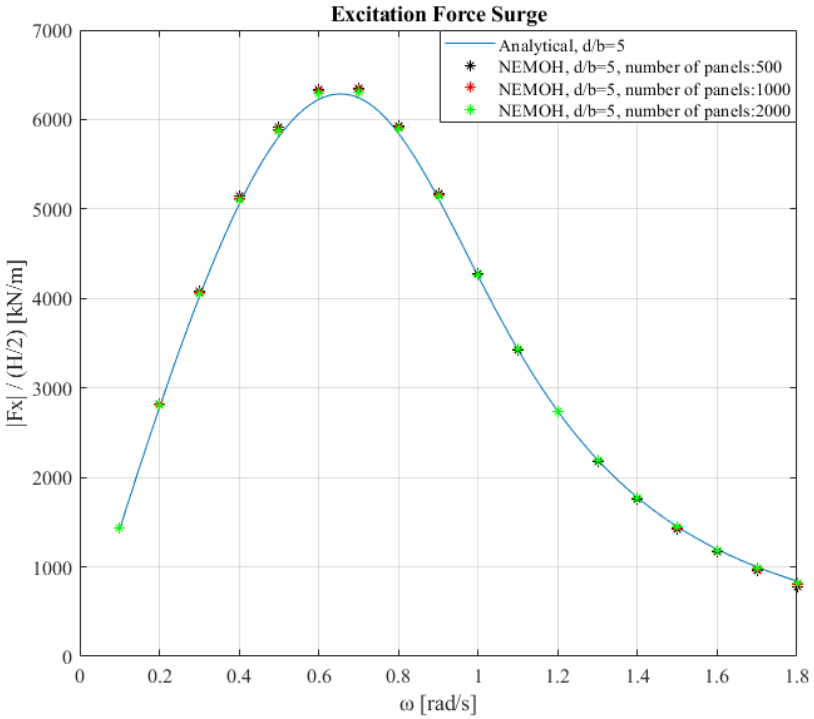

Fig. 9. Horizontal exciting force F_x versus ω for $d/b = 5$, for different numbers of body surface discretization elements for the calculations with the aim of the NEMOH.

In Fig. 9 the numerical results of the analytical solution and the open-source code NEMOH for different numbers of body surface discretization elements ($500, 1000$ and 2000), for the exciting wave force Fx are plotted against the wave angular frequency ω, for Case study 2. Considering the body surface increase, a larger number of elements for the different studied discretization cases is selected.

For wave angular frequency $0.4 < \omega < 1$ values and for wave angular frequency values ($\omega > 1.6$ rad/s) a discretization with small number of elements leads to overestimated and underestimated values of the exciting wave force Fx (compared to the corresponding analytical solution results) respectively. Therefore a total of 2000 quadrilateral elements have been used for the discretization of the body's wetted surface for ratio d/b equal to 3, in the case of the open-source code NEMOH calculations (see Fig. 3).

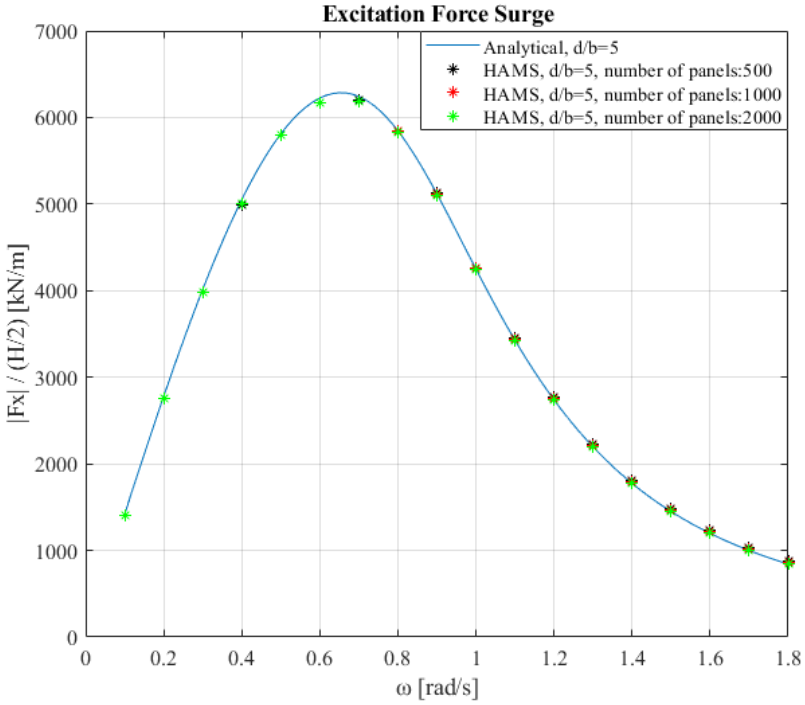

Fig. 10. Horizontal exciting force F_x versus ω for $d/b = 5$, for different numbers of body surface discretization elements for the calculations with the aim of the HAMS.

In Fig. 10 the numerical results of the analytical solution and the open-source code HAMS for different numbers of body surface discretization elements ($500, 1000$ and 2000), for the exciting wave force Fx are plotted against the wave angular frequency ω, for Case study 2. The body surface discretization cases studied in the case of the open-source code NEMOH calculations are also studied in the case of the open-source code HAMS calculations, in order to compare the computing precision of the two codes. For wave angular frequency values ($\omega > 1.6$ rad/s) a discretization with small number of elements leads to overestimated values of the exciting wave force Fx (compared to the corresponding analytical solution results). Therefore a total of 2000 quadrilateral elements have been used for the discretization of the body's wetted surface for ratio d/b equal to 5, in the case of the open-source code HAMS calculations (see Fig. 4).

In Tables 2-4 the computing speed of the open-source codes NEMOH and HAMS for each Case study and each different case of panel discretization is shown. As the number of panel discretization elements increases, the computing speed for both codes decreases. Also, in case of HAMS, the number of threads used in simulations also affects the computing speed (as the number of threads increase, the computing speed decreases). The computing speed of HAMS is significant greater than NEMOH. Both

the open-source BEM codes were run on a computer with an 11th Gen Intel® Core ™ i7 processor running at 1690 MHz using 16.0 GB RAM, running Windows version 10.

Table 2. Code computing speed for Case Study 1.

Number of panels	NEMOH	HAMS (number of threads: 1)	HAMS (number of threads: 8)
200	4.4 s	3.5 s	1 s
400	17.1 s	6.2 s	2.3 s
600	37.2 s	17.9 s	6.2 s

Table 3. Code computing speed for Case Study 2.

Number of panels	NEMOH	HAMS (number of threads: 1)	HAMS (number of threads: 8)
300	7.9 s	5.1 s	1.5 s
600	38.1 s	16.8 s	4.2 s
900	84.2 s	46.6 s	11.3 s

Table 4. Code computing speed for Case Study 3.

Number of panels	NEMOH	HAMS (number of threads: 1)	HAMS (number of threads: 8)
500	24.8 s	10 s	2.5 s
1000	110.8 s	59.8 s	14.4 s
2000	557.6 s	287.1 s	100.8 s

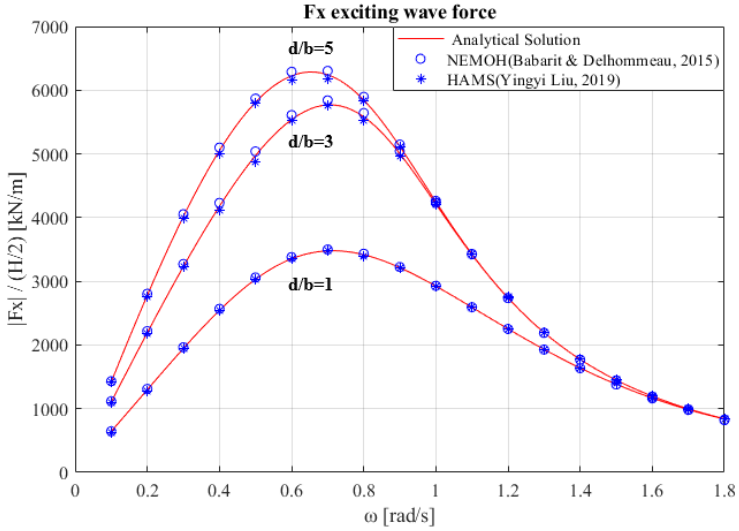

Fig. 11. Horizontal exciting force F_x versus ω.

In Fig. 11 the exciting wave force Fx, acting on the vertical cylinder is plotted as a function of the wave angular frequency ω (rad/s) for wave direction equal to 0° as shown in Fig. 1. The numerical results of the analytical solution are similar to the analytical solution of [15] and BEM methods (NEMOH and HAMS). It can be concluded that the mesh geometry resulting from the mesh parametric analysis is adequate.

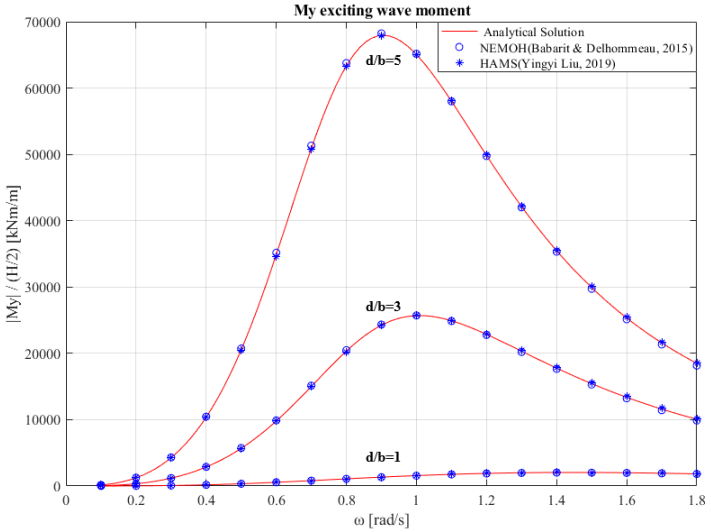

Fig. 12. Exciting moment M_y versus ω.

In Fig. 12 the moment My, acting on the vertical cylinder is plotted against the wave angular frequency ω (rad/s) for wave direction equal to 0° as shown in Fig. 1. The

moment is calculated at e_c measured from the free surface for each different cylinder case. The numerical results of the analytical solution are similar to the analytical solution of [15] and BEM methods (NEMOH and HAMS). It can be concluded that the mesh geometry resulting from the mesh parametric analysis is adequate.

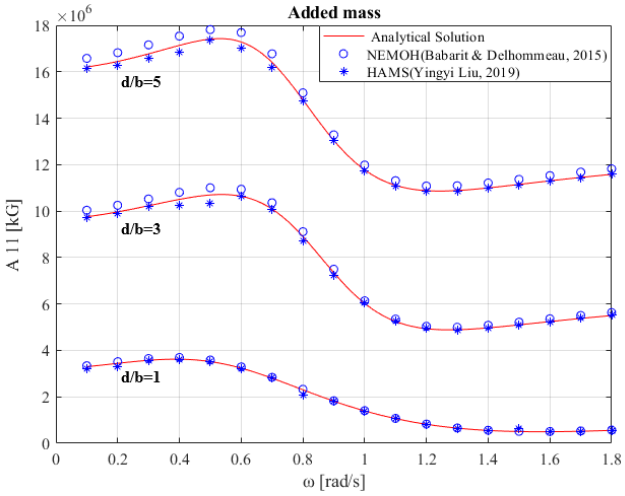

Fig. 13. A_{11} added mass versus ω.

In Fig. 13 the added mass $A_{11}$of the vertical cylinder is plotted as a function of the wave angular frequency ω (rad/s). The numerical results of the analytical solution are similar to those of the open-source codes NEMOH and HAMS and the analytical solution of [11]. It can be concluded that the mesh geometry resulting from the mesh parametric analysis is adequate.

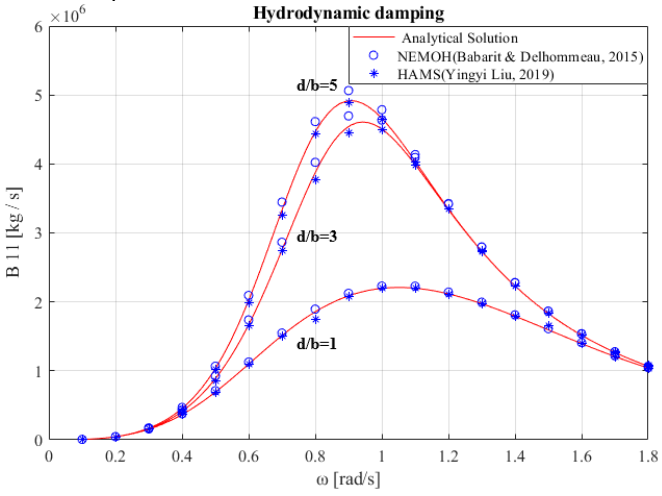

Fig. 14. B_{11} hydrodynamic damping versus ω.

In Fig. 14 the hydrodynamic damping B_{11} of the vertical cylinder is plotted as a function of the wave angular frequency ω (rad/s). The numerical results of the analytical solution are similar to those of the open-source codes NEMOH and HAMS and the analytical solution of [11]. It can be concluded that the mesh geometry resulting from the mesh parametric analysis is adequate.

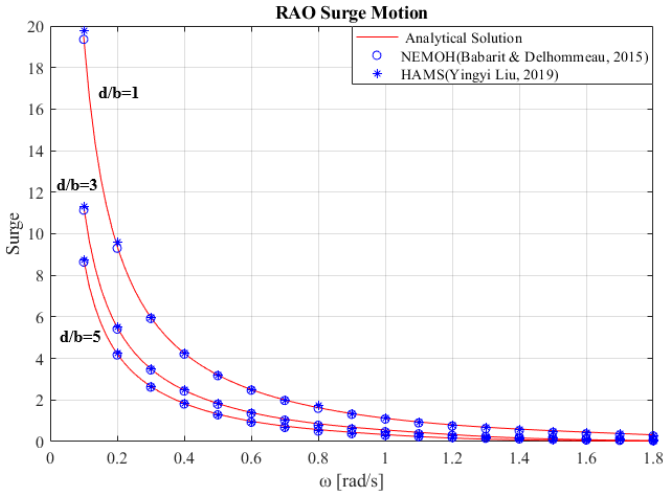

Fig. 15. RAO of the surge motion versus ω.

In Fig. 15 the RAO of the surge motion of the vertical cylinder is plotted as a function of the wave angular frequency ω (rad/s) for wave direction equal to 0^o as shown in Fig. 1. The numerical results of the analytical solution of [15] are similar to those of the BEM methods (NEMOH and HAMS). It can be concluded that the mesh geometry resulting from the mesh parametric analysis is adequate.

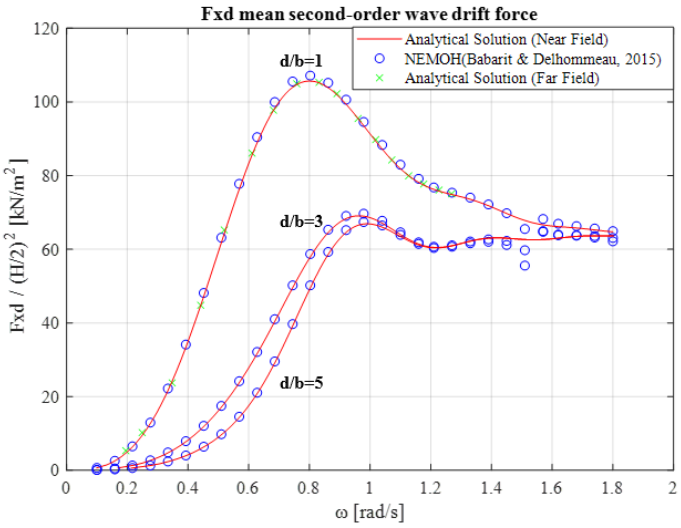

Fig. 16. Horizontal mean second-order wave drift force versus ω.

In Fig. 16 the horizontal mean second-order wave drift force acting on the vertical cylinder is plotted as a function of the wave angular frequency ω (rad/s) for wave direction equal to 0º as shown in Fig. 1. The numerical results of the analytical solution are similar to the analytical solution of [15] and to the results of the open-source code NEMOH, expect from one specific value of wave angular frequency (equals to 1.5 rad/s) which is probably an irregular frequency [25]. According to [15] the mean second-order wave drift forces give the same results when we solve the diffraction problem with the near field and far field methods. A crucial difference between the near field and far field method is the fact that the latter based on the determination of the scattered potential at a distance of the body, avoiding the determination of the velocity potential and its derivatives on body surface, although mean second-order wave drift forces are calculated in all six motions with the aim of the near field method instead of only three motions with the aim of the far field method.

Comparisons of the mean second-order wave drift force (in case of fixed bodies) for both methods (far field and near field) and both methodologies (analytical and numerical) serves as another reliable criterion to verify the mesh quality for the BEM methods [27]. The similarity in numerical results declares that the body surface discretization used in BEM methods is accurate and therefore the mesh grid parametric analysis carried on in this manuscript might be able to be avoided.

4 Conclusions

After completing the numerical procedures for the calculation of the basic hydrodynamic loads acting on the fixed cylinder, the following conclusions have been arising:

(1) The numerical results of the analytical solution are similar to those of the BEM methods. It has been shown, through the process of determined the mesh grid characteristics that an increase in the number of panels optimize the computational accuracy of the source codes based on BEM methods. Therefore, it is very useful to compare the numerical results of the source codes based on BEM methods to those of literature analytical numerical solutions, in order to make reliable estimations for the exact shape and size of the body mesh grid, an element that would possible lead to a significant decrease of the computational time.

(2) In case of the mean second-order wave drift force where the accuracy of the open-source code NEMOH is examined through analytical solutions using both the methods (far field and near field), consistency in numerical results indicates that the quality of mesh grid used in BEM methods is precise, suggesting that the mesh grid parametric analysis conducted in this study could potentially be bypassed.

(3) During the evaluation procedure with the aid of the open-source computational programs NEMOH and HAMS, it has been noticed that the computing speed of HAMS is greater than NEMOH especially when the number of threads HAMS used in its simulations is greater than one. (for example in Case study 2 HAMS needs 11.3 seconds to proceed with the numerical calculations, while NEMOH needs almost one and a half minute). This element was crucial for increasing the number of panels for discretizing a more complex cylinder-wetted surface, in order to improve the accuracy of HAMS. However, it is essential to be mentioned that NEMOH is able to calculate arrays of bodies, where HAMS in its current version only makes calculations on a single body.

(4) The next steps will be dealt with the calculation of the exciting wave forces, the exciting moments, the added mass, the hydrodynamic damping, the RAO's and the mean second-order wave drift forces of floating arrangements of multiple fixed vertical cylinders not only in case of simple harmonic wave incidents but also in case of random seas.

(5) The above analytical equations, as well as the mesh geometry information for the presented Case Studies can be used in benchmark tests of BEM programs for the evaluation of the mesh quality and the accuracy of their numerical results.

References

1. Mazarakos, T.P., Mavrakos, S.A., Soukisian, T.H.: Wave Loading and Wind Energy of a Spar Buoy Floating Wind Turbine. In: 2019 Fourteenth International Conference on Ecological Vehicles and Renewable Energies (EVER), pp. 1-7, Monte-Carlo, Monaco (2019).
2. Mazarakos, T.P., Mavrakos, S.A.: Wave–current interaction on a vertical truncated cylinder floating in finite-depth waters. Proceedings of the Institution of Mechanical Engineers, Part M: Journal of Engineering for the Maritime Environment 227(3), 243-255. (2013).
3. Haskind, M.D.: The Exciting Forces and Wetting of Ships in Waves. Izveslia Akademii Nauk S.S.S.R., Otdelenie Tekhnicheskikh Nauk 7, 65-79 (1957).
4. Maruo, H.: The drift of a body floating in waves. Journal of Ship Research 4(3) (1960).

5. Newman, J.: The exciting forces on fixed bodies in waves. Department of the Navy, DAVID TAYLOR MODEL BASIN, Hydromechanics Laboratory (1963).
6. Newman, J.: The drift forces and moment on ships in waves. Journal of Ship Research 11, 51-60 (1967).
7. Hess, J.L., Smith, A.M.O.: Calculation of non-lifting potential flow about arbitrary three-dimensional bodies. Journal of Ship Research 8(2), 22-44 (1964).
8. Garrett, C.J.R.: Wave forces on a circular dock. Journal of Fluid Mechanics 46(1), 129-139 (1971).
9. Bai, K.J.: Diffusion of oblique waves by an infinite cylinder. Journal of Fluid Mechanics 68(3), 513-535 (1975).
10. Pinkster, J.A., Oortmersen, G.van.: Computation of the first and the second order wave forces on oscillating bodies in regular waves. In: Proceedings, 2nd International Conference on Numerical Ship Hydrodynamics, pp. 136-159 (1977).
11. Rahman M., Bhatta, D.D.: Evaluation of added mass and damping coefficient of an oscillating circular cylinder. Applied Mathematics Modelling 17, 70-79 (1993).
12. Mavrakos, S.A.: Mean drift loads on multiple vertical axisymmetric bodies in regular waves. In: Proceedings of the 5th International Offshore and Polar Engineering Conference (ISOPE'95), vol. 3, pp. 547-555, The Hague, The Netherlands (1995).
13. Mansour, A.M., Williams, A.N., Wang, K.H.: The diffraction of linear waves by a uniform vertical cylinder with cosine-type radial perturbations. Ocean Engineering 29(3), 239-259 (2002).
14. Pinkster, J.A.: Mean and low frequency wave drifting forces on floating structures. Ocean. Eng. 6, 593-615 (1979).
15. Mazarakos, T.P.: Second-order wave loading and wave drift damping on floating marine structures, Ph.D. dissertation, School of Naval Architecture and Marine Engineering, Division of Marine Structures, Laboratory of Floating Structures and Mooring Systems, National Technical University of Athens, Greece (2010).
16. Babarit, A., Delhommeau, G.: Theoretical and numerical aspects of the open-source BEM solver Nemoh. In: 11th European Wave and Tidal Energy Conference (EWTEC2015) (2015).
17. Delhommeau, G.: Amelioration des performances des codes de calcul de diffraction – radiation au premier ordre. Nantes: Ecole Nationale Superleure de Mechanique de Nantes (1989).
18. Kurnia, R., Ducrozet, G., Gilloteaux, J.-C.: Second Order Difference-and Sum-Frequency Wave Loads in the Open-Source Potential Flow Solver NEMOH. In: International Conference on Offshore Mechanics and Arctic Engineering, volume 5A: Ocean Engineering (V05AT06A019) (2022). https://doi.org/10.1115/OMAE2022-79163.
19. Kurnia, R., Ducrozet, R.: Computation of Second-order Wave Loads on Floating Offshore Wind Turbine Platforms In Bi-chromatic Bi-directional Waves Using Open-Source Potential Flow Solver NEMOH. In 18èmes Journées de l'Hydrodynamique, 2022, https://jh2022.sciencesconf.org/420480.
20. Philippe, M., Combourieu, A., Peyrard, C., Robaux, F., Delhommeau, G. and Babarit, A.: Introducing Second Order Low Frequency Loads in the Open-Source Boundary Element Method Code Nemoh. In Proceedings of the 11th European Wave and Tidal Energy Conference. Sept 2015.
21. Yingyi, L.: HAMS: A Frequency-Domain Preprocessor for Wave-Structure Interactions Theory, Development, and Application. Journal of Marine Science and Engineering 7 (3) (2019).

22. Yingyi, L.: Introduction of the Open-Source Boundary Element Method Solver HAMS to the Ocean Renewable Energy Community. In: Proc. of the 14th European Wave and Tidal Energy Conference, Plymouth, UK, Sep. 5–9 (2021).
23. Mei, C.C.: The applied dynamics of ocean surface waves. New York: John Wiley & Sons (1963).
24. MacCamy, R.C., Fuchs, R.A.: Wave Forces on Piles: A Diffraction Theory. Tech. Memo No. 69, US Army (1954).
25. Faltinsen, O.M.: Sea Loads on Ships and Offshore Structures. Cambridge University Press, Ocean Technology Series (1992).
26. Linton, C.M., Evans, D.V.: The interaction of waves with arrays of vertical circular cylinders. Journal Fluid Mechanics 215, 549-569 (1990).
27. Mazarakos, T.P., Mavrakos, S.A.: Wave-Current Interaction Effects on the OC4 DeepCwind Semi-Submersible Floating Offshore Wind Turbine. Journal of Marine Science and Engineering 12(9), 1509 (2024).